OPTIMIZING LIGHT COLLECTION FROM THIN SCINTILLATORS USED IN A BETA-RAY CAMERA FOR SURGICAL USE

C. S. Levin, *L. R. MacDonald, M.P. Tornai, E.J. Hoffman, *J. Park
*Division of Nuclear Medicine & Biophysics, UCLA School of Medicine, and *Department of Physics, UCLA*

Abstract

We are developing a 1-2 cm^2 area camera for imaging the distribution of beta emitting radiopharmaceuticals at the surface of tissue exposed during surgery. The front end consists of a very thin continuous or segmented scintillator sensitive to betas (positrons or electrons) of a few hundred keV, yet insensitive to gamma rays. The light from the scintillator is piped away through clear fibers into the photon detector (PD). We report here on efforts made to optimize the light collection from < 3 mm thick plastic and $CaF_2(Eu)$ scintillators into clear fibers using experimental measurements and computer simulations.

I. INTRODUCTION

We are developing a surgical beta-ray sensitive scintillation camera for improved detection of residual malignant tissue after resection. We designed the instrument to be sensitive to positrons from an ^{18}F-labeled radiopharmaceutical (E_{max} = 635 keV), yet relatively insensitive to accompanying background annihilation photons. The imaging probe detector head consists of a low Z, low density, very thin, segmented or continuous scintillator (see Figure 1). The sensitive area of the face of the device exposed to the radioactive tissue is designed to be circular and roughly 1-2 cm^2 (1.25 cm diameter). The short range of the betas in tissue and scintillator, close proximity to the area being imaged and relatively large area of the device ensure high image resolution and high sensitivity to beta emitting tissue at the surface of the cavity. Imaging capabilities help to distinguish signal from background and allow a relatively large area to be assayed in a short amount of time.

We previously developed a prototype device for feasibility studies using a two-dimensional array of VLPCs as the photodetector [1,2]. In addition to optimizing that system we are currently developing a similar instrument utilizing a multi-anode PMT [3,4]. We report here on efforts made to optimize the light collection from scintillators for the probe front-end, using computer simulations and experimental measurements with a bialkali PMT. We emphasize that although specific scintillators and geometries are studied in this work, many of the results obtained apply to a wide variety of system designs that utilize fiber optic readout of scintillators.

A schematic of the device is shown in Figure 1. For flexibility and electrical insulation from body tissues during surgery, the light from the scintillator will be piped away from the patient through a matrix of long (~2 m), clear plastic optical fibers (not shown) into the multi-channel photon detector of choice (e.g. PMT, APD, VLPC). An intermediate fiber bundle (seen in the figure) will be used to readout the light from the scintillators and transfer it to the long bundle. This will allow for a removable front end of the camera to accommodate a variety of imaging conditions with different front end geometries.

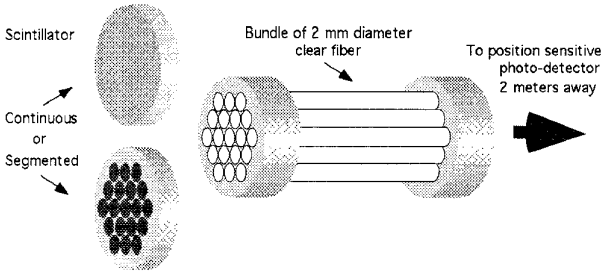

Fig. 1. Schematic of front end of the proposed Beta-Ray Camera.

II. MATERIALS AND METHODS

Positioning for the continuous scintillator version of the camera requires light sharing among the fibers, which will be accomplished with a light guide between the scintillator and fibers. The challenge of this entire approach is to transport a sufficient number of scintillation photons from the scintillator, through the two stages of clear fiber and into the photo-detector. This involves optimizing such factors as the reflector, surface treatment, and the geometry of the scintillator, choice of clear fiber, couplings between these two components and type of position sensitive photo-detector.

The choice of the low Z, low density scintillator will depend on light output and background considerations. We have focused our studies on relatively high light output plastic scintillators, such as, Bicron BC404 (un-clad, polyvinyl toluene (PVT) base) or BCF10 scintillating fiber (with clad), and $CaF_2(Eu)$. The properties of these three scintillators are shown in Table 1. The segmented detector (Fig. 1, left, bottom) is a hexagonal matrix of 19 short, 2 mm diameter scintillator disks, and the continuous detector (Fig. 1, left, top), a 1.25 cm diameter disk. Improving the light yield in plastic by increasing the fluor concentration is discussed in [5].

Light output as a function of scintillator thickness was studied for both the large and small scintillator diameters. All of the measurements were performed inside a light tight box. The thinner the scintillator, the lower the gamma-ray background, however, too thin a material will not stop the average ^{18}F positron. Since we do not want sensitivity to background annihilation gamma rays in our light yield studies, we chose an electron (^{204}Tl) rather than positron (^{18}F) beta decay source for the experiments.

Monte Carlo simulations were performed to study beta trajectories, scintillator light transmission and internal annihilation background in the scintillators of interest. The electron trajectory code was developed at UCLA, the optical

0-7803-3180-X/96$5.00©1996

Authorized licensed use limited to: Stanford University. Downloaded on June 01,2010 at 22:42:32 UTC from IEEE Xplore. Restrictions apply.

photon tracking code used was DETECT, and EGS4 was used to calculate the gamma-ray background.

Table 1. Properties of investigated low Z, low density scintillators for beta detection.

Scintil-lator	Light Output, (photons /MeV)	Max Wvlgth. Emission (nm)	Main Decay Constant (ns)	Bulk Light Attn. Length (cm)	Refractive Index	Effective Z	Density (g/cm^3)
BCF-10	8,000	432	2.7	190	1.6 core 1.49 clad	6.6	1.05
BC404	10,000	408	1.8	160	1.58	6.6	1.04
CaF_2(Eu)	17,000	435	940	~3-5	1.44	16.9	3.19

III. RESULTS

A. Monte Carlo Simulations: Electron Interactions and Background

CaF_2(Eu) has nearly a factor of two higher light output than BC404, but from Monte Carlo simulations using the EGS4 code, above a 100 keV threshold, has three times the expected gamma ray background rate (from ^{18}F positron annihilation in the scintillator and subsequent Compton scatter) than does the same size of BC404 (PVT). However, because of its higher effective Z and density, the average thickness of the CaF_2(Eu) required to stop an ^{18}F positron (E_{max} = 635 keV) is nearly one quarter of that required for PVT. The annihilation background in CaF_2(Eu) will not be as severe for thinner dimensions.

Figure 2 shows a plot of the probability that betas deposit all of their energy in the scintillator vs. scintillator thickness for ^{204}Tl and ^{18}F flood beta sources in CaF_2(Eu) and plastic using Monte Carlo simulations of positron trajectories. The thickness required to completely encompass an average beta trajectory for a flood source (normal incidence) of radiation is an upper limit for that required to stop betas entering from all

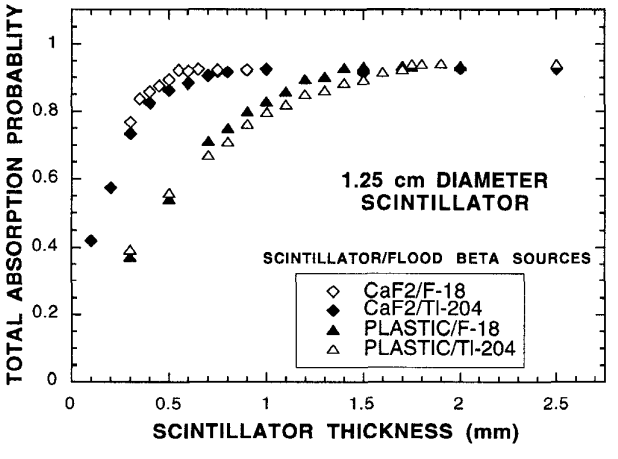

Fig. 2. Total absorption probability for beta events (trajectories) from ^{18}F and ^{204}Tl sources in CaF_2(Eu) and plastic scintillators (a 1.25 cm diameter detector is assumed).

angles. From Figure 2 it is seen that the thickness required to completely absorb greater than 90% of ^{18}F positrons is 1.3 mm and 0.5 mm for PVT and CaF_2,(Eu), respectively. This thickness is on average 10% greater for the ^{204}Tl source than for the ^{18}F source. The average range of the positrons in these materials is 0.4 and 0.16 mm, respectively, which gives an estimate of the ultimate limit of the intrinsic resolution attainable with ^{18}F beta-ray imaging in those scintillators (in our system we are "starved" for light so we want scintillator thicknesses consistent with complete absorption of the beta energy). Figure 3 shows a simulated ^{18}F positron trajectory in CaF_2(Eu). Betas continuously deposit their energy through multiple scattering with approximately 33% of the energy deposited at the end of its track, where large angle scatters occur.

B. Monte Carlo Simulations: Scintillation Light Transmission

We are fortunate in the design of the imaging array that the scintillators used are very thin. For thin scintillators where the cross-sectional area to thickness (length) ratio is high, it is much easier to collect the scintillation light from one end since the number of interactions with the sides is low. In fact, a good portion of the light may not undergo any reflections at all before exiting the scintillator.

The surface treatment of the scintillators is important. External reflectors on the back side direct the light back into the scintillator. Diffuse reflectors exhibit a Lambertian (cosθ) distribution where the reflected light is preferentially directed normal to the surface. Ground surfaces tend to break up internal reflections. Highly polished surfaces may trap some

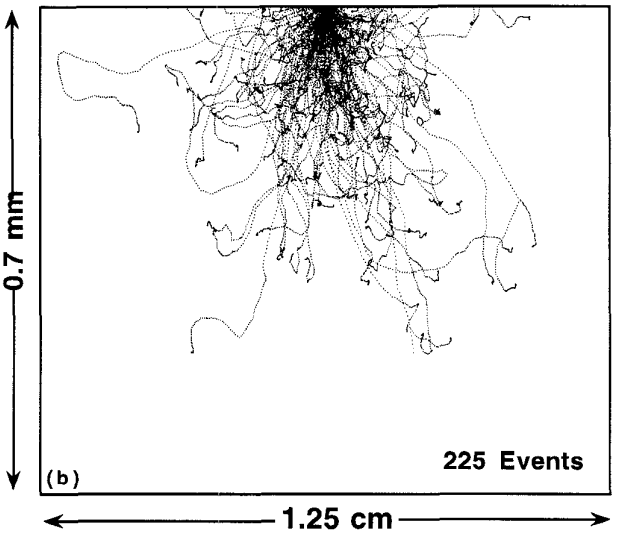

Fig. 3. Two dimensional plot (x-z) of a Monte Carlo simulation of electron trajectories for ^{18}F (E_{max} =635 keV) point source at top center of scintillator.

light due to internal reflections and this light may never enter the fiber light guides. This suggests that we may want a ground top surface with a diffuse reflector. Monte Carlo light transmission simulations were performed for various types of surfaces (ground, polished etc.) with and without several types of reflectors (paint, metal, teflon with air gap). For the continuous scintillator design, the sides will be blackened

Authorized licensed use limited to: Stanford University. Downloaded on June 01,2010 at 22:42:32 UTC from IEEE Xplore. Restrictions apply.

(absorbing) to provide uniformity of light spread for positioning [3,4]. This blackening is unnecessary for the segmented positioning situation since the scintillator-fiber units in the bundle are independent of each other. Figure 4 shows the simulated light yield obtained for various surface treatments of the scintillator top for the 2 and 12.5 mm

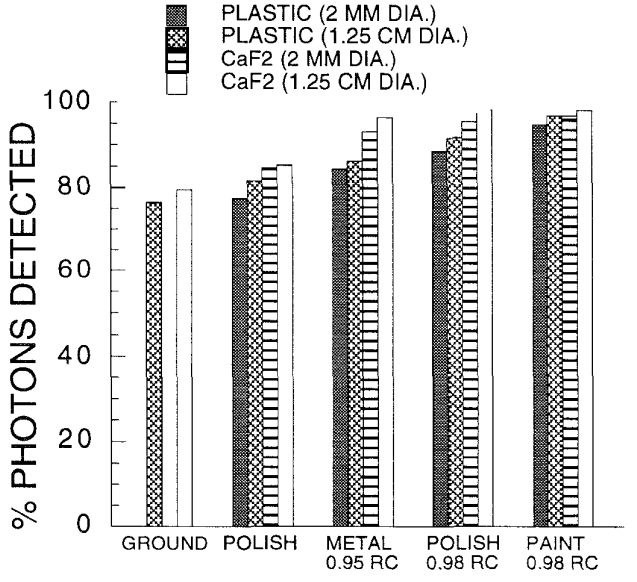

Fig. 4. Simulated scintillation light yield for various treatments of the front side of plastic and $CaF_2(Eu)$ scintillators of 1.2 and 0.7 mm thick, respectively.

diameter plastic (1.25 mm thick) and $CaF_2(Eu)$ (0.7 mm thick) scintillators. In all cases, the best conditions obtained were a slightly ground surface painted with a diffuse reflector. For the back (PMT) end of the scintillator, ground or polished surfaces tended to produce similar results.

Figure 5 shows the simulated light output for various plastic scintillator thicknesses with and without a 5 cm fiber

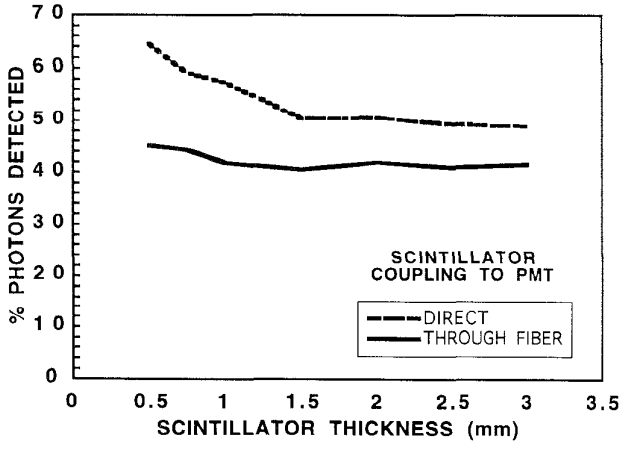

Fig. 5. Simulated light yield vs. scintillator thickness (2 mm diameter plastic or CaF_2). The clear fiber coupling (5 cm) removes the dependence of light yield on thickness.

coupled to a PMT. The scintillator was assumed to be painted with a diffuse reflector on the front and polished on the sides. There is significant difference in light transmission vs. length (as large as 30% from 0.5 to 3 mm thickness) when the scintillator is coupled directly to the PMT. The figure shows results for 2 mm diameter plastic but similar trends were found for the 1.25 cm diameter case (with and without the 19 fiber bundle) except with a less dramatic (<10%) rise for the directly coupled case. The light yield dependence on thickness in the direct coupled case is most likely due to improved angular acceptance into the PMT for thinner detectors. This variation in light collection is not seen when fiber coupling is used. The fiber effectively acts as a light collimator by only transmitting those light rays whose entrance angle meets the fiber's criteria for total internal reflection. Similar results were found with simulations using BCF10 scintillating fiber (outer clad about a scintillating core).

The light yield as a function of refractive index of the 0.1 mm thick coupling compound between the scintillator and a 5 cm long, 2 mm diameter fiber (n_{core}=1.6, n_{clad}=1.49) was also studied. The attenuation length of the fiber core and clad was set at 2 m for the simulations. Over an index of refraction range of 1.2 to 1.8 there was little variation (<10%) in yield in $CaF_2(Eu)$ and a moderate variation (<15%) for the plastic scintillator coupled to fiber. The reason for this non-intuitive weak dependence is most likely due to the finite angular cone of acceptance (numerical aperture) for the fiber. Regardless of the index of refraction of the scintillator-fiber interface, large angles of entrance into the fiber are not transmitted. Only forward directed light will be transmitted down the fiber. Thus, the index of refraction mismatch between the scintillator and fiber does not play as big a role in fiber-coupled systems.

Figure 6 shows that the amount of light detected increases with the numerical aperture (NA) of a fiber. For short fiber lengths, significant transmission of light occurs in the cladding as well as the core of the fiber. The largest NA fiber should be chosen, regardless of the value of n_{core}.

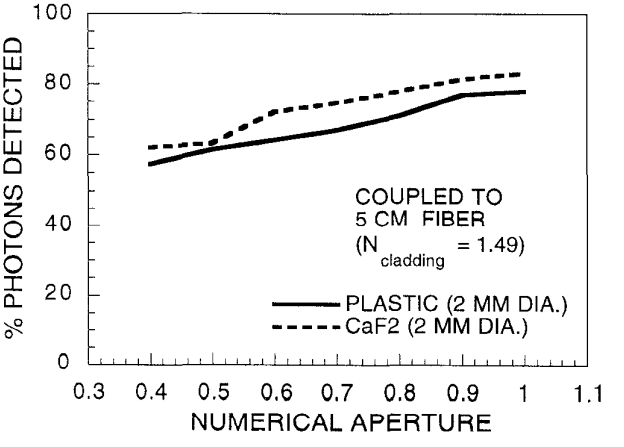

Fig. 6. Scintillation light yield when coupled to a 5 cm long clear fiber as a function of the numerical aperture of the core of the fiber.

The thickness of the light guide required for image uniformity in the continuous camera was determined [3,4] to be approximately 2 mm. The presence of a light guide introduces an extra coupling interface between the continuous scintillator and fiber bundle. The refractive index of the light guide was studied and we found that it should be high (~ 1.6) for best transmission. Assuming a polystyrene light guide (n=1.58) the light yield did not change significantly with

Authorized licensed use limited to: Stanford University. Downloaded on June 01,2010 at 22:42:32 UTC from IEEE Xplore. Restrictions apply.

refractive index of the coupling interface between the scintillator and light guide. The index of refraction of the interface between light guide and fiber was more important. The optical transmission was studied for several choices of light guides (quartz, glass and polystyrene) as a function of the refractive index of the second (light guide/fiber) interface (n = 1.5 was assumed at the scintillator light guide interface). The best response was obtained at a refractive index between 1.5 and 1.6. The low index of refraction of $CaF_2(Eu)$ (n=1.44) facilitates optical coupling to a light guide (n=1.58) and optical fiber (n=1.6 core).

Another factor that was studied was the use of various holders for the fiber bundle (see Fig. 1). The best light output was obtained using white Lucite as the material. Aluminum and black Lucite holders produced 15 and 30% lower yield, respectively. This aspect is discussed in more detail in [4].

C. Experimental Data: Scintillators for the Segmented Imaging Array

We used the weighted mean (centroid) of a ^{204}Tl beta spectrum (E_{max} = 765 keV, similar to that of ^{18}F, without the annihilation photons) as a measure of the light output of the scintillator. Figures 7 and 8 show the results of light output measurements performed using 2 mm diameter pieces of the plastic scintillator, coupled either directly onto a 5 cm

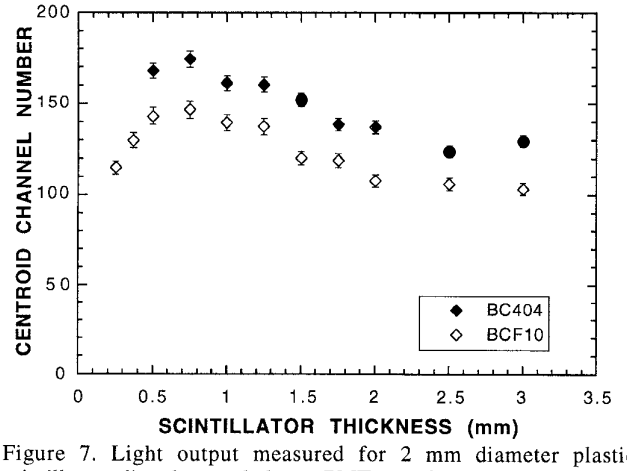

Figure 7. Light output measured for 2 mm diameter plastic scintillators directly coupled to a PMT as a function of scintillator thickness for flood beta irradiation from ^{204}Tl.

diameter PMT, or indirectly through a 5 cm long piece of 2 mm diameter clear fiber (Pol. Hi.Tech, NA = 0.57). Each point represents the mean and standard deviation of at least four separate measurements. For these initial studies no reflectors were used. For the scintillator directly coupled to the PMT (Fig. 7), the light yield increases systematically as the thickness of the scintillator decreases, until approximately 1.0 mm, where it begins to decrease (there is a 30% difference in light output between the 0.75 and 3 mm thicknesses). When coupled to the PMT through the clear fiber (Fig. 8), the thicknesses dependence of the light yield is removed since there is only roughly a 42° light acceptance cone for internally reflected light (determined by the fiber numerical aperture) and, hence, solid angle effects due to proximity are removed. These results compare well to the Monte Carlo study shown in Section IIIB, Figure 5 down to approximately 0.75 mm.

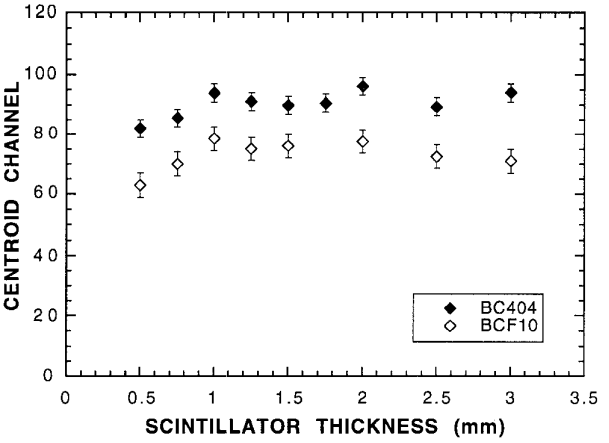

Figure 8. Light output measured for 2 mm diameter plastic scintillators coupled via a 5 cm length of clear fiber to a PMT as a function of scintillator thickness.

The competing effect of incomplete energy deposition begins to play a role at thicknesses near and below 1.0 mm, where the light output begins to decrease. Below 0.7 mm thickness we observed a rapid drop in light output due to beta penetration. The light output increase and saturation near 1.0 mm thickness in Figure 8 matches our predictions of positron range from UCLA beta trajectory/energy deposition Monte Carlo studies of Section IIIA.

There was a factor of 4.4 difference in light output measured between direct and fiber coupling to the PMT (Figures 7 and 8 have a factor of 2.5 difference in scale; the amplifier gain setting was 2.5 times higher for the data taken in Figure 8). The difference between direct and fiber coupling was not so drastic in the simulations of Figure 5. This discrepancy might be explained by the fact that perfect surfaces were assumed in the simulations. In reality the surfaces have flaws and non-uniformities.

From Figures 7 and 8 it is also seen that BC404 has systematically 20-25% more light output than the BCF 10 scintillating fiber of the same outer diameter for these short thicknesses. This corresponds to the intrinsically higher light output in the PVT base than for Polystyrene (see Table 1) and the absence of the clad and therefore larger effective cross-sectional area of the PVT. $CaF_2(Eu)$ was unavailable in the 2 mm diameter dimension for comparison.

D. Experimental Data: Scintillators for the Continuous Imaging Detector

For the continuous scintillator studies, we will consider only fiber coupling. Figure 9 shows the results measured for 1.25 cm diameter disks of BC404 and $CaF_2(Eu)$ coupled to a hexagonal-packed bundle of nineteen, 2 mm diameter clear fibers (Bicron BCF-98) for different top reflectors. For BC404, the light output varies with thickness in a similar manner to that seen in Figure 8, while for $CaF_2(Eu)$ the saturation appeared near 0.5 mm (only 3 $CaF_2(Eu)$ thicknesses were available). We measured that the $CaF_2(Eu)$ system produced on average three times the light of BC404. This is consistent

Authorized licensed use limited to: Stanford University. Downloaded on June 01,2010 at 22:42:32 UTC from IEEE Xplore. Restrictions apply.

with the differences in light output and index of refraction between $CaF_2(Eu)$ and BC404 (see Table I). The low index of refraction of $CaF_2(Eu)$ facilitates coupling to the clear plastic fiber (NA=0.57).

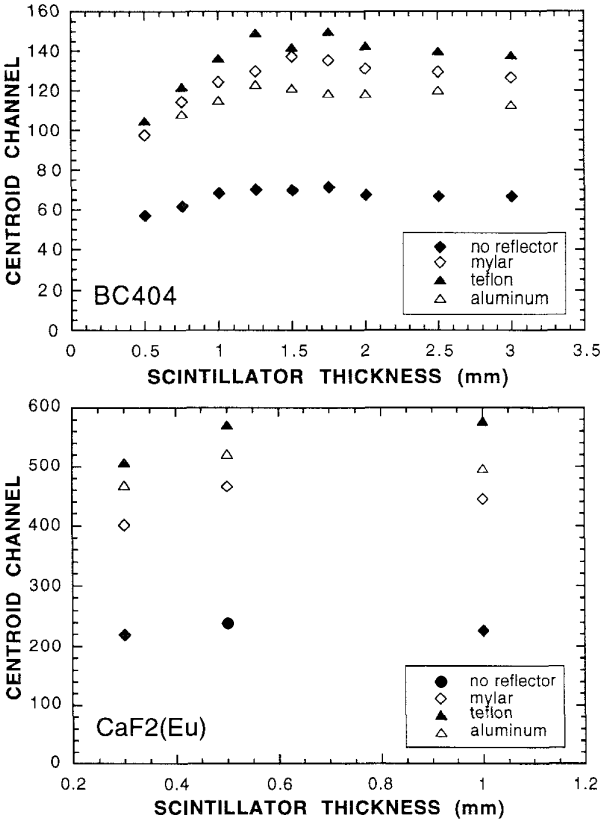

Fig. 9. Measured ^{204}Tl spectrum centroid as a function of scintillator thickness for 1.25 cm diameter (top) BC404 and (bottom) $CaF_2(Eu)$ scintillators coupled to a 19 fiber bundle of 19, 5 cm long 2 mm diameter clear plastic fibers for different top surface reflectors. The two data sets are plotted on the same scale.

As predicted from DETECT simulations (Section IIIB), the best reflector found was a white diffuse reflector (Teflon) which produced nearly twice the light output than for the case without reflectors. TiO_2 reflecting paint produced only slightly greater light output than that measured using teflon.

After calibration with an LED (described in [5]) we found that the continuous $CaF_2(Eu)$/fiber system produced on average >200 photoelectrons at the PMT photocathode for the ^{204}Tl electron spectrum. This number of photons is sufficient for < 1 mm positioning using multi-channel photodetectors. Transmission properties of quartz, glass and plastic fibers with various numerical apertures (NA) were also studied [4]. We found a double clad Kuraray fiber (NA = 0.72) to produce the best combination of high light output and sensitivity.

IV. DISCUSSION AND CONCLUSION

Because of this fiber-coupled design it is crucial that as many scintillation photons be collected by the photodetector as possible. Due to the small thicknesses of the scintillators required for beta detection, light collection efficiency from the scintillator into the fiber bundle is high.

Energy deposition and light transmission were seen to compete with one another for thin scintillator thicknesses. From our measurements we saw that fiber coupling reduces the dependence of scintillation light yield on thickness (provided the beta is sufficiently absorbed). White reflecting paint with 0.98 reflectivity produced the best scintillation light signal and it is simple to use. A clear plastic fiber (Kuraray, NA=0.72) was chosen for the front end fiber readout of the scintillator. For the continuous scintillator imaging probe polystyrene (n=1.6) was chosen for the light guide.

Whether one uses a continuous or segmented scintillator for the camera depends on several considerations. Because of higher coupling efficiency to the fibers, the light yield and energy resolution for the segmented array, with 19 independent scintillator-fiber units is higher. However, in that case the image resolution (pixel size) is determined by the diameter of each individual scintillator unit in the array, in this case 2 mm. One may then want to reduce the scintillator diameter, which means increasing the number of elements in the array in order to cover the same imaging area, which in our prototype design is 1.2 cm^2 (~1.25 cm total scintillator diameter). However, the scintillator diameter should not be smaller than that required to stop the average beta.

With the continuous positioning camera, the positioning is accomplished through light sharing among the fibers in the bundle (the fibers are, thus interdependent) and a weighted mean of the individual fiber signals. In principle, the image resolution is limited only by the number of scintillation light photons produced and distributed into the fibers in the bundle and we have observed 0.5 mm [4] resolution (significantly better than the 2 mm diameter clear fiber size). In addition, because of the lower packing fraction in the segmented array (unless square pieces are used) the overall efficiency and sensitivity is better for the continuous scintillator.

V. REFERENCES

[1] LR MacDonald, MP Tornai, CS Levin, J Park, M Atac, DB Cline and EJ Hoffman. Investigation of the Physical Aspects of Beta Imaging Probes Using Scintillating Fibers and Visible Light Photon Counters. *IEEE Trans. Nucl. Sci.* **42-4**, August 1995, 1351-7.

[2] LR MacDonald, MP Tornai, CS Levin, J Park, M Atac, DB Cline and EJ Hoffman. Small area, fiber coupled scintillation camera for imaging beta-ray distributions intra-operatively. Presented at *SPIE*, July 1995 (in press).

[3] MP Tornai, CS Levin, LR MacDonald, EJ Hoffman, J Park, M Atac. Development of a Small Area Beta Detecting Probe for Intra-Operative Tumor Imaging. *J. Nucl. Med.* **36**, 1995, p. 109. Presented at the Society of Nuclear Medicine Conference, June 1995.

[4] MP Tornai, LR MacDonald, CS Levin, S. Siegel, EJ Hoffman. Design Considerations and Performance of a 1.2 cm^2 Beta Imaging Intra-operative Probe. Presented at *IEEE Medical Imaging Conference*, October, 1995.

[5] MP Tornai, EJ Hoffman, CS Levin, LR MacDonald. Optimization of Fluor Concentration in a New Organic Scintillator for In Situ Beta Imaging. Presented at *IEEE Medical Imaging Conference*, October, 1995.

The authors thank Ken Meadors for technical assistance. This research was supported by NIH Grants T32 CA09092 and R01-CA56655, DOE Grant DE-FC03-87-ER 60615 and the Whitaker Foundation.

Authorized licensed use limited to: Stanford University. Downloaded on June 01,2010 at 22:42:32 UTC from IEEE Xplore. Restrictions apply.